VSP Journal of Adhesion Science and Technology 23 (2009) 1515–1530
Journal of ADHESION SCIENCE and TECHNOLOGY
www.brill.nl/jast

Observations of Decreased Fracture Toughness for Mixed Mode Fracture Testing of Adhesively Bonded Joints

David A. Dillard [a,*], **Hitendra K. Singh** [a], **David J. Pohlit** [a,**] **and J. Michael Starbuck** [b]

[a] Engineering Science and Mechanics Department Virginia Tech, Blacksburg, VA 24061-0219, USA
[b] Polymer Matrix Composites Group, Material Science & Technology Division Oak Ridge National Laboratory, Oak Ridge, TN 37831-6053, USA

Abstract
In contrast to fracture in monolithic materials, where cracks naturally grow in a mode I manner, fracture in laminated or adhesively bonded joints often involves cracks growing under mixed mode conditions. In many cases, the mixed mode fracture energy increases as the fracture mode changes from mode I to mode II, but exceptions have been noted for several practical engineering adhesives. In some cases, $\mathcal{G}_{\mathrm{IIc}}$ may be less than $\mathcal{G}_{\mathrm{Ic}}$, while in other situations, failure may occur at total energy release rate ($\mathcal{G}_{\mathrm{T}} = \mathcal{G}_{\mathrm{I}} + \mathcal{G}_{\mathrm{II}}$) values that are smaller than either of the pure mode fracture energies. Several examples of this behavior are reported along with possible explanations for the behavior, which often involves the propagation of the growing debond into regions where less energy is dissipated by the fracture process. These examples showing that mixed mode fracture energies of adhesive joints may be lower than pure mode fracture energies remind us of the importance of developing fracture envelopes over a wide range of mode mixities for engineering design.

Keywords
Mixed mode fracture, adhesive bonds, crack path selection, fracture envelopes

1. Introduction

In the fracture of isotropic monolithic materials, cracks will turn or kink to propagate in a mode I fashion [1, 2]. Several criteria have been suggested to describe this phenomenon, including that fracture proceeds in the direction where the stresses are maximum [3], that fracture grows in the direction that maximizes the energy release rate [4], and that fracture proceeds such that the crack grows in a manner that the mode II stress intensity factor is zero, $K_{\mathrm{II}} = 0$ [1, 5]. The predictions from all three of these different criteria are generally in very good agreement with each other and with experimental observations [6]. The ability to predict crack path

* To whom correspondence should be addressed. Tel.: 540-231-4714; Fax: 540-231-4574; e-mail: dillard@vt.edu
** Currently at the Naval Surface Warfare Center — Carderock Division, Bethesda, Maryland 20817, USA

 DOI:10.1163/156856109X452701

selection has matured into a robust and accurate methodology, at least in materials that behave in a linear elastic fashion [7, 8]. Because of the propensity for cracks to grow in a mode I fashion in monolithic materials, fracture tests for such materials typically focus on mode I loading, although initiation of fracture under mixed mode loading is also of interest. Mode mixity ψ may be defined in terms of ratios of the shear to opening stress intensity factors or energy release rates, $\psi = \tan^{-1} K_{\mathrm{II}}/K_{\mathrm{I}} = \tan^{-1}\sqrt{\mathcal{G}_{\mathrm{II}}/\mathcal{G}_{\mathrm{I}}}$. This definition for mode mixity is appropriate for fracture of monolithic materials, and as such is often used for cohesive fractures within adhesive layers of bonded joints.

Researchers have long recognized that fracture processes become more complex in layered materials, such as laminated composites and adhesively bonded joints, where the presence of planes or regions with different mechanical properties means that cracks, forced to grow between the tougher layers, often initiate and propagate under mixed mode conditions. Nonetheless, fracture testing for such materials is perhaps most commonly performed in mode I loading for several reasons, including: (1) mode I loading is often the simplest to perform (mode I fracture typically induces smaller stresses in adherends, thereby reducing likelihood of adherend failure [9], opening mode cracks are easier to see and measure, and the test fixtures are often simpler and more widely available); (2) mode I fracture energies are often believed to be smaller than fracture energies measured in other (especially pure) modes, thus leading to conservative designs; and (3) perhaps this focus is a holdover from the mode I failures and studies that dominate fracture in monolithic materials. Nonetheless, the need for characterizing the fracture energies under mode II and mode III loading, as well as some mixed mode testing, has long been recognized [10].

For interfacial fracture, there is strong evidence that fracture energies are smallest when opening or mode I conditions prevail. In careful experiments conducted by Liechti and Liang [11, 12] spanning a wide range of mode mixities, the interfacial fracture energy of a glass/epoxy system was shown to be smallest over the range of interfacial mode mixity of $\psi = 0$ to 40°, where $\psi = \tan^{-1}\{\mathrm{Im}[Kh^{i\varepsilon}]/\mathrm{Re}[Kh^{i\varepsilon}]\}$ [13]. The fracture energy increased substantially for $\psi > 40°$ and even more dramatically for negative values of ψ. Here K is the complex interfacial stress intensity factor, h is a characteristic length, ε is the bimaterial constant, and Re and Im denote the real and imaginary components, respectively. (For interfacial fracture, the asymmetry allows for the shear portion of the stress intensity factor to be either positive or negative, corresponding with either opening or closing contributions to the fracture, which tends to bias the effect depending on the sign of ψ.) They also demonstrated that long range tractions were more likely explanations for the fact that measured normal crack opening displacements were consistently smaller than predicted values, rather than either plastic dissipation or asperity shielding mechanisms. The asymmetric shielding was successfully modeled by including hydrostatic and rate effects in models of the fracture zone [14–16]. Wang and Suo [17]

have experimentally demonstrated similar dependence on mode mixity for Plexiglas/epoxy bonds using Brazil nut specimens. Tang *et al.* [18] were able to predict similar experimental trends for mode mixity by analyzing nonlinear viscous dissipation contributions.

The above studies were for relatively brittle systems, so fracture energies were typically below 100 J/m^2. The dependence of the measured fracture energy on mode mixity may become more complex when dealing with engineering applications of structural adhesives formulated to exhibit enhanced mechanical properties. This paper will briefly review mixed mode test methods and describe results from several engineering adhesive applications that exhibit significant reductions in fracture energy as mode mixity increases from opening mode to in-plane shearing mode. Of particular interest is that in at least some cases, relatively small fractions of mode II loading are able to significantly change the locus of failure and reduce the fracture energy dramatically. Such results suggest the need for a thorough evaluation of mixed mode fracture energies to obtain relevant system properties for engineering design, as failure to recognize the reduced fracture energies could lead to nonconservative designs. Although mode III contributions to mixed mode testing are also of interest, this paper will focus on the in-plane fracture modes involving mode I and mode II fracture only.

2. Fracture Tests for a Range of Mode Mixity

A large number of fracture specimens have been proposed or adapted for the study of debonding of adhesively bonded joints and the closely related delamination of laminated materials. Mostovoy and Ripling [19] were perhaps the first to develop test methods for fracture of adhesive bonds, using both the double cantilever beam (DCB) and tapered double cantilever beam (TDCB) specimens to characterize the mode I fracture energy, the latter of which had the advantage that the applied energy release rate at constant load was nominally independent of the crack length. Another early test geometry, the cracked lap shear (CLS) specimen, was proposed by Brussat *et al.* [20]. This specimen offers a mixed mode global fracture energy that, for identical adherends, has a mode mixity of about 49°, although this can be varied over a modest range by varying the relative stiffness of the lap and strap adherends. This specimen was especially popular in fatigue testing in the aircraft industry [21], in part because the available strain energy release rate is nominally independent of crack length at fixed load, although some deviations do exist [22]. Because this specimen is loaded in tension rather than in bending, a different loading apparatus is needed. A number of other specimens that are dominantly loaded in bending have been developed, including the mixed mode bend or fixed ratio flex specimen, perhaps more uniquely described as the single leg bend (SLB) specimen [23], which for identical adherends results in a mode mixity of $\tan^{-1}\sqrt{3/4}$. Pure mode II tests include the end notch flex (ENF) and end load split (ELS) configu-

Table 1.
Illustration of various loading configurations with their mode mixity

Test configuration	Test samples	Global mode mixity, Ψ
Double cantilever beam (DCB)	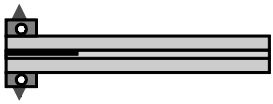	0°
Asymmetric double cantilever beam (ADCB)	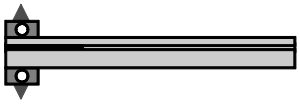	0–34°
Single leg bend (SLB)	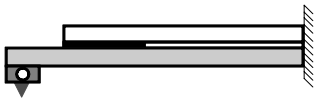	41°
Cracked lap shear (CLS)	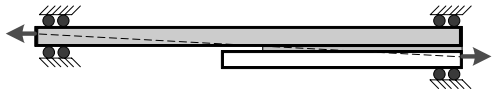	49°
End load split (ELS)	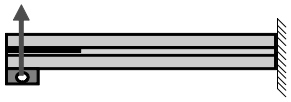	90°
End notch flex (ENF)	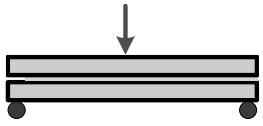	90°

rations, which produce similar crack tip loading but involve different test fixturing. Table 1 illustrates these loading modes along with their mode mixity.

The mode mixities for all of these specimens can be varied significantly by adjusting the relative stiffness (thickness and/or modulus) of the two adherends. Suo and Hutchinson [24] and Williams [25, 26] have provided useful relationships for cracks in both monolithic and bimaterial systems that describe the fracture energies and mode mixities for the general case of a cracked object, the legs of which are loaded by axial forces and moments [24, 27]. Although the variation in mode mixity with adherend stiffness differences can be quite pronounced in monolithic or bilayer systems, the effect is significantly mitigated for the case of a softer adhesive layer bonding two adherends [28]. Thus the local mode mixity can be significantly different than the globally applied mode mixity.

Part of the difficulty with obtaining a complete fracture envelope for bonded adhesive joints and laminated composites is that no single test specimen or loading fixture is sufficient to characterize the full range of in-plane fracture. Each spec-

imen configuration requires a different fracture analysis method, many of which have been enhanced to correct for a variety of complications that enter the testing. In an effort to provide a range of mode mixity using a common specimen and loading fixture, Reeder and Crews [29, 30] developed a fixture for studying a range of mode mixities for laminated composites. This geometry has also been adapted to mixed mode fracture studies of adhesively bonded joints. Fernlund and Spelt [31, 32] proposed an alternate geometry for conducting a range of mode mixity tests on standard beam specimens. These fixtures have the advantage in that they can be used in a standard axial load frame, but practical limitations may include the range of mode mixity achieved, the time required to adjust the mode mixity, the size which may limit the ability to conduct environmental tests, and the difficulty of using these fixtures in fatigue loading. One possibility for varying the mode mixity over a limited range with the same specimen and loading configuration is to vary the relative stiffness of the adherends. Park and Dillard [28], for example, have proposed a hybrid tapered cantilever beam configuration in which one adherend has a constant cross section and the other adherend is a typical TDCB configuration. As the crack grows, the mode mixity changes over a modest range (for example, in the acrylic adhesive to aluminum bonded specimens reported, the local mode mixity ranged from 0° to about 20°). Modified Arcan tests using precracked specimens have also been used to provide a range of fracture mode mixities simply by changing the pin locations on the Arcan fixture [33, 34].

A range of mode mixities can be obtained by using test frames equipped with dual actuators that may be independently controlled to adjust the mode mixity. Several examples of these are reported in the literature, although their cost and special nature make them limited in their availability. Dillard *et al.* [35] have developed a dual actuator load frame with horizontally mounted hydraulic actuators. The uncracked end of a standard DCB specimen is fixed in a clamp at the base, and the two actuators are attached to the debonded legs of the specimen. By varying the loads or displacements applied to the ends of the specimen, any in-plane mode mixity can be obtained, even within a single test specimen. Although dual actuator devices such as this are not likely to become common due to their specialized nature, they do offer unique opportunities for characterizing a wide range of issues related to various mode mixity loadings.

3. Mixed Mode Fracture Criteria

Mixed mode fracture energy results may be presented in several ways, including as plots of total fracture energy as a function of mode mixity and as fracture envelopes in which either stress intensity factors (K) or strain energy release rates ($\mathcal{G}$) for mode I and mode II loading are plotted on the abscissa and ordinate axes, respectively. This latter form is used herein, as it lends itself to direct comparisons of the

fracture energies. Functional forms have been used to express the fracture energy criteria such as [36]:

$$\left[\frac{(\mathcal{G}_{\mathrm{I}})_{\mathrm{c}}}{\mathcal{G}_{\mathrm{Ic}}}\right]^{\alpha} + \left[\frac{(\mathcal{G}_{\mathrm{II}})_{\mathrm{c}}}{\mathcal{G}_{\mathrm{IIc}}}\right]^{\beta} = 1, \tag{1}$$

where $(\mathcal{G}_{\mathrm{I}})_{\mathrm{c}}$ and $(\mathcal{G}_{\mathrm{II}})_{\mathrm{c}}$ are the mode I and mode II components of the strain energy release rate at fracture, $\mathcal{G}_{\mathrm{Ic}}$ and $\mathcal{G}_{\mathrm{IIc}}$ are the critical fracture energies for pure modes, and α and β are exponents. Since $K_{\mathrm{I}} = \sqrt{\overline{E} \cdot \mathcal{G}_{\mathrm{I}}}$ and $K_{\mathrm{II}} = \sqrt{\overline{E} \cdot \mathcal{G}_{\mathrm{II}}}$, where $\overline{E} = E$ for plane stress conditions and $\overline{E} = E/(1 - \nu^2)$ for plane strain conditions, E is Young's modulus of the adhesive and ν is Poisson's ratio, the related expression for the stress intensity factors can be written as:

$$\left[\frac{(K_{\mathrm{I}})_{\mathrm{c}}}{K_{\mathrm{Ic}}}\right]^{2\alpha} + \left[\frac{(K_{\mathrm{II}})_{\mathrm{c}}}{K_{\mathrm{IIc}}}\right]^{2\beta} = 1. \tag{2}$$

The exponents may be chosen to form the best fit of experimental data or may be prescribed based on some assumed relationship. For example, if the critical fracture energy is assumed to depend only on the total fracture energy ($\mathcal{G}_{\mathrm{T}} = \mathcal{G}_{\mathrm{I}} + \mathcal{G}_{\mathrm{II}}$) and not the mode mixity, $\alpha = \beta = 1$ and $\mathcal{G}_{\mathrm{Ic}} = \mathcal{G}_{\mathrm{IIc}}$. This results in squaring the stress intensity terms in equation (2), which being proportional to stress, provides a fracture criterion that is similar to the von Mises yield criterion. If α and β are both greater than or equal to unity, the resulting criterion implies that the mixed mode fracture energies will be larger than the minimum of $\mathcal{G}_{\mathrm{Ic}}$ and $\mathcal{G}_{\mathrm{IIc}}$. In that case, the use of the minimum pure mode fracture energy ($\mathrm{Min}(\mathcal{G}_{\mathrm{Ic}}, \mathcal{G}_{\mathrm{IIc}})$) would be conservative for design purposes [33]. On the other hand, if α is less than unity, mixed mode fracture energies could be smaller than $\mathcal{G}_{\mathrm{Ic}}$, which is often the smallest pure mode fracture energy.

Alternate forms for fracture envelope criterion have also been proposed [37, 38], including [39]:

$$\left(\frac{\mathcal{G}_{\mathrm{I}}}{\mathcal{G}_{\mathrm{Ic}}} - 1\right)\left(\frac{\mathcal{G}_{\mathrm{II}}}{\mathcal{G}_{\mathrm{IIc}}} - 1\right) - I_i\left(\frac{\mathcal{G}_{\mathrm{I}}}{\mathcal{G}_{\mathrm{Ic}}}\right)\left(\frac{\mathcal{G}_{\mathrm{II}}}{\mathcal{G}_{\mathrm{IIc}}}\right) = 0. \tag{3}$$

This relationship involves a single interaction factor, I_i, which is zero if there is no interaction ($\mathcal{G}_{\mathrm{I}}/\mathcal{G}_{\mathrm{Ic}} = 1$ or $\mathcal{G}_{\mathrm{II}}/\mathcal{G}_{\mathrm{IIc}} = 1$, corresponding to $\alpha \to \infty$ and $\beta \to \infty$) and unity if there is a simple addition ($\mathcal{G}_{\mathrm{I}}/\mathcal{G}_{\mathrm{Ic}} + \mathcal{G}_{\mathrm{II}}/\mathcal{G}_{\mathrm{IIc}} = 1$, corresponding to $\alpha = \beta = 1$) such that the total energy release rate controls the fracture. Cases of interest in this paper, where the interaction reduces the fracture energy, correspond with $I_i < 1$.

In real bonds, criterion such as given above may be used to model fracture envelopes, but because they are phenomenological in nature, they typically cannot accurately represent results when changes in locus or type of fracture process occur. Mechanistically, shear stresses tend to drive cracks away from a path that is parallel to the bond planes, potentially steering cracks into regions of the material

system where the energy dissipation associated with crack advance can change significantly [40, 41]. In some cases, the direction of the shear stress state in relation to the growing crack can steer the crack towards interfaces that are 'weaker', allowing the crack to propagate with less energy dissipation. In other cases, however, the crack can actually be steered to regions where greater energy dissipation occurs because of an improved interface [42] or other reasons. To understand the role that shear stress plays in determining the mode of failure, note that in homogeneous isotropic materials, cracks tend to propagate perpendicular to the direction of maximum tensile stress. In an adhesive joint subjected to a shear state, cracks within the adhesive layer have a tendency to grow toward one interface. Shear-dominated loading often results in interfacial failures or failures with less adhesive left on an interface [41–45], although more complex hackle pattern failures have also been reported [46]. Also, some adhesive fracture envelopes are relatively smooth, permitting reasonable fits with phenomenological criteria, such as cited above. Where changes in failure mode occur, however, the fracture envelopes may take on distorted shapes, as reported in the following section.

4. Results of Representative Adhesive Systems

As mentioned above, an increase of the fracture energy with increasing mode-mixity phase angle is generally found when the crack is located at an interface [47–49] and can be attributed to factors such as the roughness of the crack surfaces, the presence of residual stresses, crack tip shielding, and the mismatch of elastic properties at the interface [50]. Similar increases of fracture energy with increasing ψ are also often seen in engineering systems, as has been reported by many investigators for laminated composites and for adhesively bonded joints [28, 48]. Here, the rise may be phenomenologically attributed to two factors: that $\mathcal{G}_{\mathrm{IIc}}$ typically exceeds $\mathcal{G}_{\mathrm{Ic}}$, for reasons cited earlier, and that the interaction of fracture modes under mixed mode loading often has only little detrimental effect on measured fracture energies. For a common class of elastic–plastic materials [51], the yield envelopes (plots of multi-axial stress or strain) are convex, but no such requirement exists for fracture envelopes obtained under mixed mode conditions. In many cases, however, the interaction has relatively benign effects on the mixed mode fracture energy, and fracture energies often fall near or above the simple sum of the normalized components:

$$\left[\frac{(\mathcal{G}_{\mathrm{I}})_{\mathrm{c}}}{\mathcal{G}_{\mathrm{Ic}}}\right]+\left[\frac{(\mathcal{G}_{\mathrm{II}})_{\mathrm{c}}}{\mathcal{G}_{\mathrm{IIc}}}\right]=1. \tag{4}$$

Liechti and Freda [52] showed a significant increase in fracture energy in going from mode I to mode II fracture in aluminum joints bonded with scrim-supported Cytec FM-300 epoxy (Cytec Engineered Materials, Havre de Grace, MD), but on the other hand showed that mixed mode fracture occurred at slightly lower fracture energies than predicted by equation (4). Mild to modest detrimental interactions have also been reported for the global interlaminar fracture energies of

carbon/epoxy composites [38] and steady state fracture propagation in polyether sulfone (PES) composites [53]. Exceptions to both the general trends for $\mathcal{G}_{IIc} > \mathcal{G}_{Ic}$ and a relatively benign interaction for mixed mode fracture have been seen, however, including observations from our group that will be summarized in this section.

In studies of a phenylethynyl-terminated polyimide (PETI-5) adhesive used to bond titanium adherends, the mode II fracture energy, $\mathcal{G}_{IIc}$, was found to be only 52% of the value obtained for $\mathcal{G}_{Ic}$ [54]. Using asymmetric DCB and single leg bend (SLB) specimens, intermediate fracture energies were obtained for mixed mode loading. The significant drop in fracture energy in mode II loading was attributed to a pronounced change in the locus of failure. Whereas mode I loading resulted in fractures propagating along the midplane of the adhesive layer, mode II loading drove the failure to the interface with one of the adherends, a common effect of shear loading in adhesive joints. The adhesive layer for this system incorporated a polyimide film supported on a woven fiberglass scrim cloth, as is commonly used in the aircraft industry as a carrier and for controlling bondline thickness. The mode I fracture surfaces revealed failures of the adhesive being ripped from the scrim yarn interface, resulting in tortuous failure paths that involved significant evidence of plastic yielding and perhaps a limited amount of fiber bridging. As the mode mixity was increased, the locus of failure gradually shifted out of the dissipative midplane region, resulting in mixed failure regions, as shown in Fig. 1. Figure 2 shows the fracture envelope generated over a range of test configurations.

In a second example, a rubber toughened epoxy was used to bond aluminum adherends. Increasing the mode mixity through the use of several test geometries

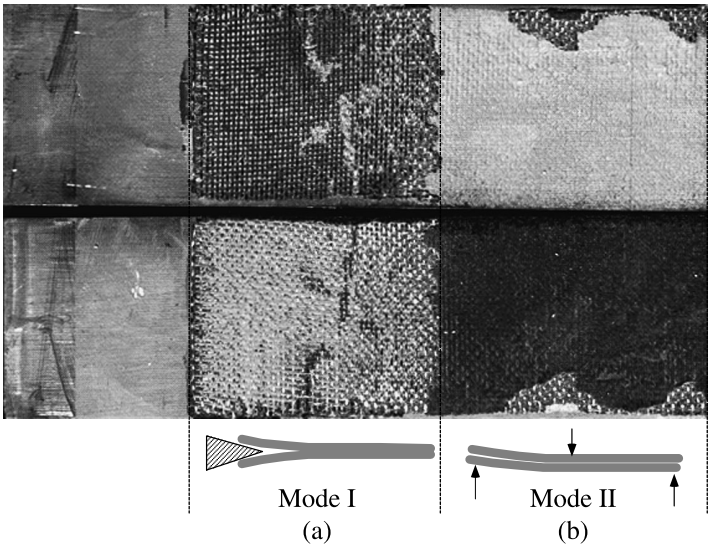

Figure 1. Locus of failure for (a) mode I and (b) mode II loaded regions of titanium adherends bonded with a polyimide adhesive film supported on a fiberglass scrim cloth.

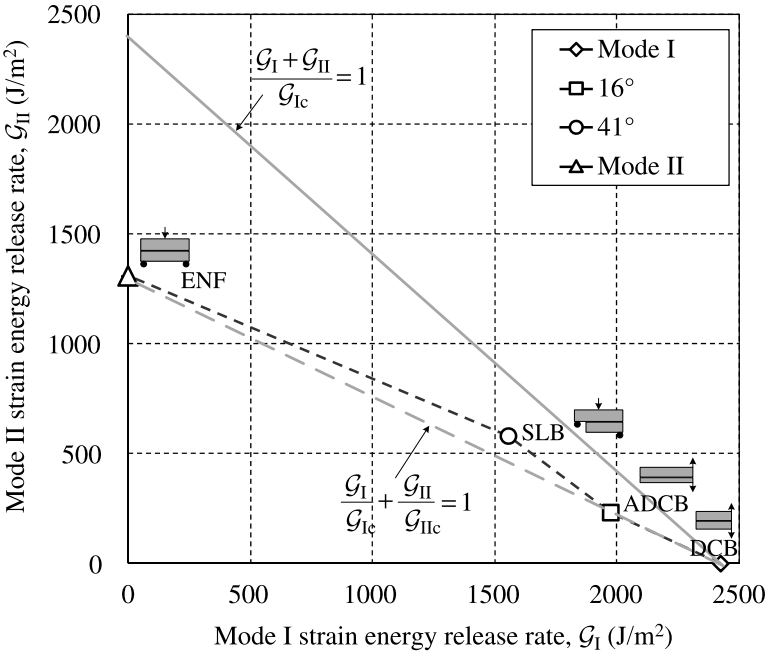

Figure 2. Fracture envelopes for titanium adherends bonded with a polyimide adhesive.

resulted in a steady decrease in fracture energy [42, 55]. Atomic force microscope (AFM) examination of the fracture surfaces revealed that increasing proportions of mode II loading had driven the locus of failure towards the interface with the adherend undergoing more tensile bending stress at the bonded surface. The fracture toughness measured decreased as the mode II fracture component increased. Owing to the toughening mechanism associated with the presence of rubber particles in the bulk of the adhesive, more energy was consumed when the crack propagated within the adhesives than along the interface. Also of interest with this system was a study of the effect of varying the quality of the surface pretreatment of one adherend relative to the other, effectively producing 'better' and 'worse' interfaces. In spite of the presence of the inferior interfaces, mechanical shear loading was capable of driving the crack along the 'better' interfaces, in a convincing example that cracks do not always propagate at the 'weakest' location in continuous systems such as adhesive joints. Figure 3 shows the fracture envelope generated over a range of test configurations, along with images of the fracture surfaces.

As a third example, the case of fracture of bonded wood specimens has shown reduced fracture energies when small proportions of mode II loading are added to predominantly mode I loading situations. In a recent study [56], southern yellow pine specimens were bonded with a polyurethane adhesive. As shown in Fig. 4, a very pronounced drop in fracture energies was observed, although the cause is not completely understood. In the polyimide and epoxy systems mentioned above,

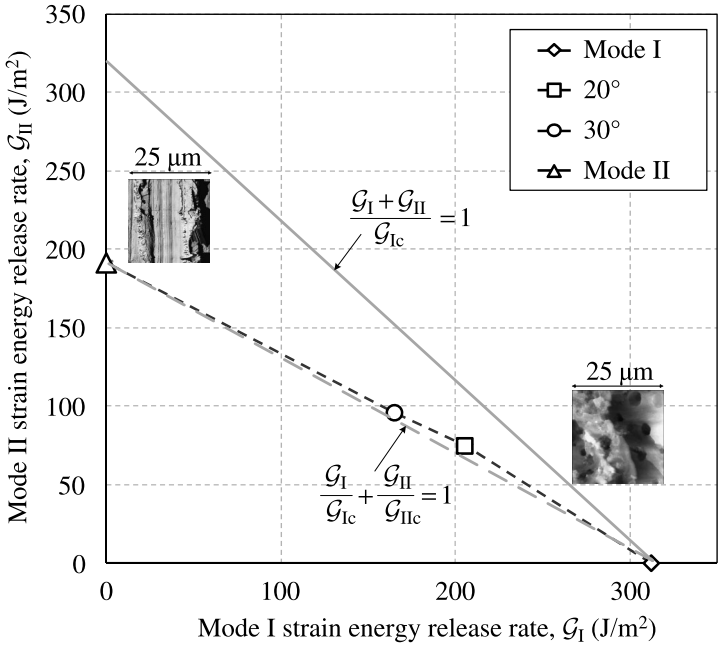

Figure 3. Fracture envelopes for aluminum adherends bonded with a rubber toughened epoxy.

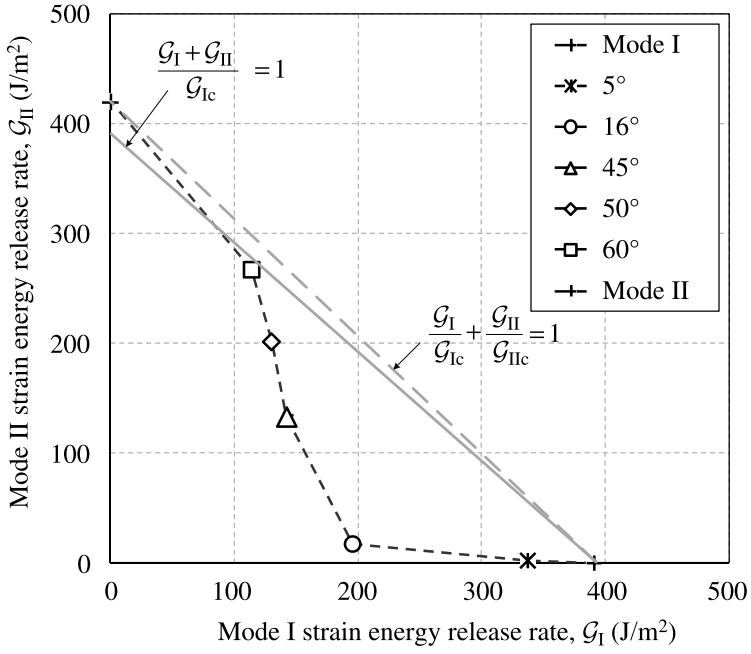

Figure 4. Fracture envelopes for southern yellow pine (*pinus spp*) adherends bonded with a polyurethane adhesive.

the mode II loading created a shear stress at the crack tip that tended to drive the crack towards the interface with the adherend surface under larger tensile strain. In these systems, at least, the energy dissipation associated with fracture near the interface was less than present within the bulk of the adhesive bond, leading to reduced fracture energies. In the case of the wood bonds, this explanation is not as convincing, as the adhesive layer is very thin and the locus of failure was not noticeably different as the mode mixity was increased.

Finally, recent testing of a 2-part commercially available epoxy (PL-731-SI provided by Sovereign Speciality Chemicals, Inc., Buffalo, NY) has revealed particularly dramatic variations in the measured fracture energies as a function of mode mix. In compact tension tests on the neat adhesive, a substantial drop in the mode I fracture toughness, K_{Ic}, was observed as the rate of testing was increased or as the temperature decreased [57]. This significant rate dependence manifests itself in pronounced stick–slip behavior when testing aluminum [58] and composite adherend [58–60] DCB specimens. Significant adhesive plasticity was evident in the form of stress-whitened beach marks separated by 50 to 100 mm. The enhanced plasticity forming at these arrest regions results in significant fracture energies, $\mathcal{G}_{\mathrm{Ic}}$, as high as 2500 J/m^2, which are quite substantial for an epoxy adhesive. The $\mathcal{G}_{\mathrm{IIc}}$ values obtained by testing bonded end load split (ELS) specimens were considerably higher. However, small to moderate proportions of mode II loading drove the cracks out of the midplane region of the adhesive layer, where large scale yielding was possible, forcing the debond to grow near an interface and significantly reducing the fracture energies one would report. Total fracture energies as small as 34% of $\mathcal{G}_{\mathrm{Ic}}$ were measured. Figure 5 illustrates the disappearance of the stress-whitened zones from the fracture surfaces with increasing mode mixity. Mode II loading permitted only a single fracture energy to be measured, as the failure was quickly driven to an interlaminar failure within the composite adherend. The resulting fracture envelope is shown in Fig. 6.

5. Discussion

Of particular interest is the abrupt drop in the total fracture energy as small proportions of mode II loading are applied, i.e., the total value of fracture energy does not remain constant as mode mixity changes but is reduced to a value significantly lower than observed for either pure mode I or mode II conditions. This observation is clearly seen in Fig. 7, a normalized fracture energy plot as a function of ψ for several adhesively bonded systems, where mixed mode fracture energies can be as low as 25% of $\mathcal{G}_{\mathrm{Ic}}$. This is an important point to consider because designing adhesively-bonded structures using only the mode I and mode II critical strain energy release rate (SERR) values could be nonconservative. To simplify design, using the lowest fracture energy within the anticipated range of applied mode mixities may be appropriate. By measuring fracture energies of bonded specimens over a range of mixed

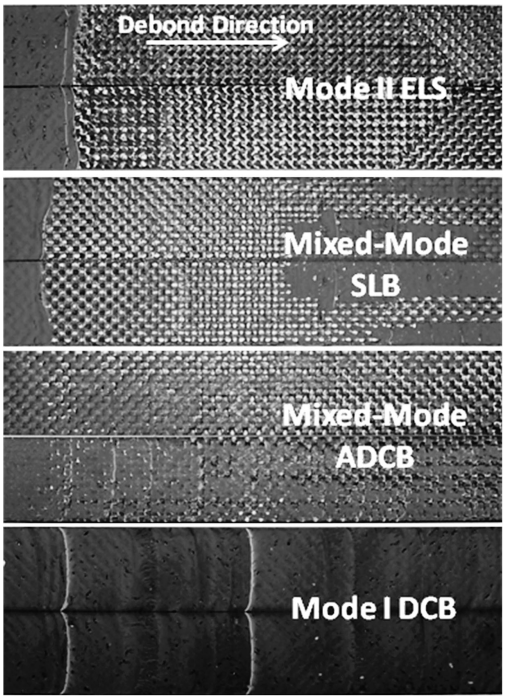

Figure 5. Illustration of locus of failure resulting from a range of applied fracture modes for composite adherends bonded with epoxy adhesive.

mode loading conditions and generating the corresponding fracture envelope, conservative estimates may be provided while designing bonded structures subjected to mixed-mode loading conditions.

Another interesting point in each of the cases cited above is that the crack could be steered away from the less energy dissipative interface region and into the central region of the bondline where additional plasticity or crack path tortuosity resulted in enhanced fracture energies. This clearly contradicts the common wisdom that failures occur at the weakest link. This old adage may apply to discrete items, such as links in a chain, but does not directly apply to continuous materials. Failure is to be viewed as the spatially varying stress field in front of the dominant crack tip interacting with the material's spatially varying resistance to fracture. The stress state is a tensor quantity, as is the resistance to fracture in some systems, so there are both spatial and directional variations in both the induced stress and the fracture resistance.

6. Summary and Conclusions

Although mode I fracture tests are the basis of characterization of monolithic materials, mixed mode fracture is of importance in adhesively bonded joints and other

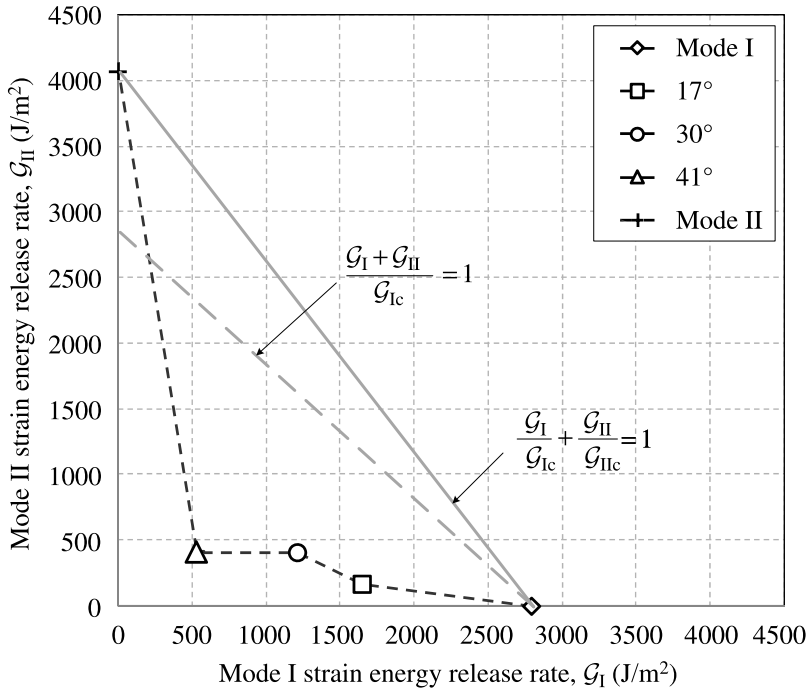

Figure 6. Fracture envelopes for composite adherends bonded with a 2-part commercially available epoxy.

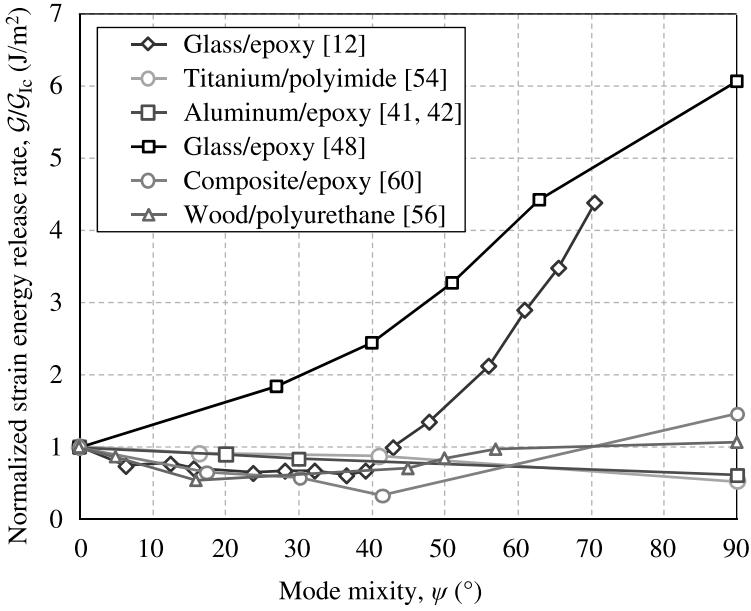

Figure 7. Examples of variation of fracture energies as a function of mode mixity for a range of adhesively bonded systems.

laminated materials because cracks are often constrained to grow within the adhesive layer. Mode I fracture tests remain of primary importance even for these bonded materials, but a number of tests have been proposed and are used to characterize mode II and III fracture, as well as combined mode mixities of all three modes, but especially for in-plane loading (combinations of modes I and II). These tests can allow for the construction of fracture envelopes that span mode mixities of interest for design or other applications. Although increasing proportions of mode II loading often result in increased fracture energies for a variety of reasons, in some cases, substantial drops in fracture energies can result. This paper presents several cases, involving commercial adhesives, in which the fracture energies drop significantly when small proportions of mode II loading are added to predominantly mode I loading conditions, resulting in complex fracture envelopes. These drops in fracture energy likely result from a change in the locus of failure, in which the growing debond is driven, by the shear stress state, to a region in which less energy is required to propagate the crack. Of particular concern from a design perspective is that in certain material systems, modest proportions of mode II loading can reduce the fracture energies below those obtained for mode I loading, which is often thought to result in the lowest fracture energies. The results remind us that mode I loading does not always result in a minimum fracture energy, and that use of mode I fracture energy values is not always conservative in design.

Acknowledgements

The authors would like to acknowledge the support of the National Science Foundation (DMR NSF 0415840) in the development of a dual actuator load frame capable of facilitating mixed mode fracture studies. The support of the Automotive Composites Consortium Energy Management Group is also acknowledged. The authors also acknowledge that a portion of this research is supported, in part, by the Department of Energy cooperative agreement number DE-FC05-95OR22363. Such support does not constitute an endorsement by the Department of Energy of the views expressed herein.

References

1. B. Cotterell and J. R. Rice, *Int. J. Fract.* **16**, 155 (1980).
2. D. Xie, A. M. Waas, K. W. Shahwan, J. A. Schroeder and R. G. Boeman, *CMES–Comput. Model. Eng. Sci.* **6**, 515 (2004).
3. V. F. Erdogan and G. C. Sih, *Trans. ASME J. Basic Eng.* **85**, 519 (1963).
4. K. Palaniswamy and W. G. Knauss, *Mech. Today* **4**, 87 (1978).
5. R. V. Goldstein and R. L. Salganik, *Int. J. Fract.* **10**, 507 (1974).
6. P. H. Geubelle and W. G. Knauss, *ASME J. Appl. Mech.* **61**, 560 (1994).
7. T. N. Bittencourt, P. A. Wawrzynek, A. R. Ingraffea and J. L. Sousa, *Eng. Fract. Mech.* **55**, 321 (1996).

8. R. G. Pettit, C. S. Chen, A. R. Ingraffea and C. Y. Hui, *Eng. Fract. Mech.* **68**, 1181 (2001).
9. Y. H. Lai and D. A. Dillard, *Int. J. Solids Struc.* **34**, 509 (1997).
10. G. P. Anderson, S. J. Bennett and K. L. DeVries, *Analysis and Testing of Adhesive Bonds*. Academic Press, New York, NY (1977).
11. K. M. Liechti and Y. M. Liang, *Int. J. Fract.* **55**, 95 (1992).
12. Y. M. Liang and K. M. Liechti, *Int. J. Solids Struc.* **32**, 957 (1995).
13. J. R. Rice, *ASME J. Appl. Mech.* **55**, 98 (1988).
14. J. G. Swadener and K. M. Liechti, *ASME J. Appl. Mech.* **65**, 25 (1998).
15. J. G. Swadener, K. M. Liechti and A. L. de Lozanne, *J. Mech. Phys. Solids* **47**, 223 (1999).
16. J. G. Swadener, K. M. Liechti and Y. M. Liang, *Int. J. Fract.* **114**, 113 (2002).
17. J. S. Wang and Z. Suo, *Acta Metall. Mater.* **38**, 1279 (1990).
18. S. Tang, T. F. Guo and L. Cheng, *Int. J. Solids Struc.* **45**, 2493 (2008).
19. S. Mostovoy and E. J. Ripling, *Fracturing Characteristics of Adhesive Joints*. Air Force Materials Laboratory, Wright-Patterson Air Force Base, Dayton, OH (1972).
20. T. R. Brussat, S. T. Chiu and S. Mostovoy, *Fracture Mechanics for Structural Adhesive Bonds*. Air Force Materials Laboratory, Wright-Patterson Air Force Base, Dayton, OH (1977).
21. W. S. Johnson, G. P. Anderson, L. P. Abrahamson, K. L. DeVries, T. R. Brussat, B. Dattaguru, P. D. Mangalgiri, F. Erdogen, P. Joseph, R. A. Everett, J. D. Whitcomb, W. L. Hufferd, G. E. Law, C. J. Lof and S. Mall, *J. Test. Eval.* **15**, 303 (1987).
22. Y. H. Lai, M. D. Rakestraw and D. A. Dillard, *Int. J. Solids Struct.* **33**, 1725 (1996).
23. B. D. Davidson and V. Sundararaman, *Int. J. Fract.* **78**, 193 (1996).
24. Z. G. Suo and J. W. Hutchinson, *Int. J. Fract.* **43**, 1 (1990).
25. J. G. Williams, *J. Strain Anal. Eng. Des.* **24**, 207 (1989).
26. J. G. Williams, *Compos. Sci. Technol.* **35**, 367 (1989).
27. J. W. Hutchinson and Z. Suo, *Adv. Appl. Mech.* **29**, 63 (1992).
28. S. Park and D. A. Dillard, *Int. J. Fract.* **148**, 261 (2007).
29. J. R. Reeder and J. H. Crews, *J. Compos. Technol. Res.* **14**, 12 (1992).
30. J. R. Reeder and J. H. Crews, *AIAA J.* **28**, 1270 (1990).
31. G. Fernlund and J. K. Spelt, *J. Compos. Technol. Res.* **16**, 234 (1994).
32. G. Fernlund and J. K. Spelt, *Compos. Sci. Technol.* **50**, 441 (1994).
33. N. Choupani, *Eng. Fract. Mech.* **75**, 4363 (2008).
34. J. L. Högberg, B. F. Sørensen and U. Stigh, *Int. J. Solids Struct.* **44**, 8335 (2007).
35. D. A. Dillard, H. K. Singh, S. Park, D. Ohanehi and M. A. McGaw, in: *2006 Society for Experimental Mechanics Annual Conference & Exposition*. Society for Experimental Mechanics, St. Louis (2006).
36. A. J. Russel and K. N. Street, in: *STP 876 Delamination and Debonding of Materials*, W. S. Johnson (Ed.), p. 349. ASTM, Philadelphia (1985).
37. A. J. Kinloch, *Adhesion and Adhesives: Science and Technology*. Chapman and Hall, London (1987).
38. M. Charalambides, A. J. Kinloch, Y. Wang and J. G. Williams, *Int. J. Fract.* **54**, 269 (1992).
39. S. Hashemi, A. J. Kinloch and J. G. Williams, *J. Mater. Sci. Lett.* **8**, 125 (1989).
40. H. Chai, *Exp. Mech.* **32**, 296 (1992).
41. B. Chen, D. A. Dillard, J. G. Dillard and R. L. Clark, *Int. J. Fract.* **114**, 167 (2002).
42. B. Chen, D. A. Dillard, J. G. Dillard and R. L. Clark, *J. Adhesion* **75**, 405 (2001).
43. B. Chen and D. A. Dillard, *Int. J. Adhesion Adhesives* **21**, 357 (2001).
44. B. Chen and D. A. Dillard, *Int. J. Solids Struct.* **38**, 6907 (2001).

45. C. S. Chen, R. Krause, R. G. Pettit, L. Banks-Sills and A. R. Ingraffea, *Int. J. Fract.* **107**, 177 (2001).
46. H. Chai, *Int. J. Fract.* **32**, 211 (1986).
47. A. R. Akisanya and N. A. Fleck, *Int. J. Fract.* **58**, 93 (1992).
48. F. Ducept, P. Davies and D. Gamby, *Int. J. Adhesion Adhesives* **20**, 233 (2000).
49. T. Ikeda, N. Miyazaki and T. Soda, *Eng. Fract. Mech.* **59**, 725 (1998).
50. R. Duer, D. Katevatis, A. J. Kinloch and J. G. Williams, *Int. J. Fract.* **75**, 157 (1996).
51. P. M. Naghdi and J. A. Trapp, *Mech. Eng.* **97**, 101 (1975).
52. K. M. Liechti and T. Freda, *J. Adhesion* **28**, 145 (1989).
53. S. Hashemi, A. J. Kinloch and J. G. Williams, *Compos. Sci. Technol.* **37**, 429 (1990).
54. H. Parvatareddy and D. A. Dillard, *Int. J. Fract.* **96**, 215 (1999).
55. B. Chen and D. A. Dillard, in: *Adhesion Science and Engineering — I: The Mechanics of Adhesion*, D. A. Dillard and A. V. Pocius (Eds), p. 389. Elsevier Science, Amsterdam (2002).
56. H. K. Singh, A. Chakraborty, C. E. Frazier and D. A. Dillard, in: *Proc. 31st Annual Meeting of the Adhesion Society*, K. M. Liechti (Ed.). The Adhesion Society, Blacksburg, VA (2008).
57. D. J. Pohlit, D. A. Dillard, G. C. Jacob and J. M. Starbuck, *J. Adhesion* **84**, 143 (2008).
58. J. C. Simón, E. Johnson and D. A. Dillard, *J. ASTM Int.* **2**, 53 (2005).
59. D. A. Dillard, G. C. Jacob and J. M. Starbuck, in: *Proc. 29th Annual Meeting of the Adhesion Society*. The Adhesion Society, Blacksburg, VA (2006).
60. D. J. Pohlit, D. A. Dillard, J. M. Starbuck and G. C. Jacob, in: *Proc. 30th Annual Meeting of the Adhesion Society*. The Adhesion Society, Blacksburg, VA (2007).